JOURNAL OF VIROLOGY, June 2006, p. 5599–5610 Vol. 80, No. 11
0022-538X/06/$08.00+0 doi:10.1128/JVI.01773-05

Silencing of Hepatitis A Virus Infection by Small Interfering RNAs

Yuri Kusov,[1]* Tatsuo Kanda,[2] Ann Palmenberg,[3] Jean-Yves Sgro,[3] and Verena Gauss-Müller[1]

Department of Medical Molecular Biology, University of Lübeck, Lübeck, Germany[1]; Health Science Center and Department of Medicine and Clinical Oncology, Graduate School of Medicine, Chiba University, Chiba, Japan[2]; and Institute for Molecular Virology, University of Wisconsin, Madison, Wisconsin[3]

Received 23 August 2005/Accepted 14 March 2006

Infection by hepatitis A virus (HAV) can cause acute hepatitis and, rarely, fulminant liver failure, in particular in patients chronically infected with hepatitis C virus. Based on our previous observation that small interfering RNAs (siRNAs) can silence translation and replication of the firefly luciferase-encoding HAV replicon, we now exploited this technology to demonstrate the effect of siRNAs on viral infection in Huh-7 cells. Freshly and persistently infected cells were transfected with siRNAs targeting various sites in the HAV nonstructural genes. Compared to a single application, consecutive siRNA transfections targeting multiple sequences in the viral genome resulted in a more efficient and sustained silencing effect than a single transfection. In most instances, multiple applications of a single siRNA led to the emergence of viral escape mutants with mutated target sites that rendered these genomes resistant to RNA interference (RNAi). Efficient and sustained suppression of the viral infectivity was achieved after consecutive applications of an siRNA targeting a computer-predicted hairpin structure. This siRNA holds promise as a therapeutic tool for severe courses of HAV infection. In addition, the results provide new insight into the structural bases for sequence-specific RNAi.

Hepatitis A virus (HAV) has a single-stranded RNA genome of 7.5 kb with positive polarity. As a member of the picornavirus family, it is unique in its biological properties, in particular, in its highly protracted replicative cycle in cell cultures and inability to shut off the host cell metabolism. HAV causes a self-limiting infection of the liver with usually mild or no symptoms in young patients, whereas adult patients might suffer from severe symptoms. In immune-compromised or chronically infected patients, fulminant hepatic failure is often associated with a high mortality rate (15, 52). Albeit vaccines against hepatitis A virus can prevent the disease (3, 14, 31), they are futile for fulminant hepatitis. Therefore, therapeutic intervention strategies to prevent progression to a life-threatening liver disease are still in need. Given that the rapid degradation of the HAV genome can ameliorate viral infection and thus prevent fulminant failure, RNA interference (RNAi) based on sequence-specific genome degradation may present a novel and specific therapeutic approach in preventing severe disease progression.

Initially demonstrated in *Caenorabditis elegans* and *Drosophila melanogaster*, RNAi is now recognized as a valuable tool to silence viral infections (reviewed in references 22, 48, and 50). Among the numerous viruses that have been successfully silenced by RNAi, there are five representatives of the picornavirus family: poliovirus (19, 20), human rhinovirus (45), enterovirus 71 (37), foot-and-mouth disease virus (7, 9, 36), and coxsackievirus B3 (1, 40). Recently, we have shown that genome replication of an HAV replicon can be efficiently inhibited by small interfering RNAs (siRNAs) targeting either coding or noncoding regions of the genome (26, 27, 34). Yet, silencing of the complete HAV life cycle by RNAi has so far not been addressed, owing to several unique features of this virus that might conflict with efficient gene silencing. The noncytolytic replication of HAV in cell culture is unusual for a picornavirus, yet typical for other hepatitis viruses, such as hepatitis B virus and hepatitis C virus (HCV), for which successful RNAi has been reported (4, 18, 30, 50). In contrast to most picornaviruses, HAV replicates asynchronously in cell culture due to the highly protracted uncoating of the viral RNA. The HAV capsid differs from that of other picornaviruses in its high physical stability, which efficiently protects the genome from degradation. This feature and the relative long half-life of the viral genome may hamper the efficacy of short-lived siRNAs (35). Finally, due to the high mutation rate during RNA virus replication, the HAV genome has the potential to escape the siRNA inhibitory pressure with the emergence of resistant mutants.

Various approaches have been tested to efficiently and sustainably interfere with viral replication, including siRNA-expressing vectors and multiple siRNA applications. In general, however, the sequence and/or structural motifs of an individual siRNA and its target still remain elusive. Hence, to more efficiently suppress HCV and poliovirus replication, multiple sequences within the viral genome have been targeted using endonuclease-generated siRNAs (21, 30). In order to reduce nonspecific effects on cellular genes, unique and, possibly, conserved sequences in the viral genome should be targeted.

In the experimental setting of the HAV-infected cell culture, we elaborated molecular details to efficiently interfere with HAV replication. We used various siRNAs that target sequences within the region encoding the HAV nonstructural proteins and that had been successfully shown to inhibit replication of the HAV replicon (26, 34). Although specific and sustained suppression by siRNAs was observed, their efficiency

* Corresponding author. Mailing address: Institute of Medical Molecular Biology, University of Lübeck, Ratzeburger Allee 160, 23562 Lübeck, Germany. Phone: 49-451-5004085. Fax: 49-451-5003637. E-mail: koussov@molbio.uni-luebeck.de.

and the emergence of RNAi-resistant mutants varied significantly and depended on the amount of actively replicating viral genomes present under various infection conditions. Comparing the viral escape genomes, evidence was obtained that RNAi-resistant genomes either preexisted in the quasispecies populations of the viral inoculum or emerged by mutation under the siRNA selection pressure. We identified an exceptionally efficient siRNA target (2C-1) in the HAV gene 2C that significantly reduced the viral infectious titer without giving way to measurable viral escape mutants. Unlike the other siRNA targets, computer folding of the entire HAV genome predicts the 2C-1 target assumes a hairpin conformation. Our data suggest that RNAi may provide a specific antiviral approach to treat severe cases of hepatitis A.

MATERIALS AND METHODS

Cells and viruses. African green monkey kidney (BS-C-1) cells and the human hepatoma cells (Huh-7) (41) were grown in Dulbecco's modified minimal essential medium (DMEM) supplemented with 2 mM glutamine, 100 U/ml penicillin, 100 μg/ml streptomycin, and fetal calf serum (10% in growth and 2% in maintenance medium). HAV inoculum derived from recombinant cDNA pT7-18f (32) was used to infect the cells at a multiplicity of infection (MOI) of 0.1 50% tissue culture infective doses ($TCID_{50}$)/cell. Huh-7 cells persistently infected with HAV (Huh-7/HAV) were prepared by consecutive passages (five times every fifth day) of HAV-infected cells as described previously for human embryo fibroblasts (51).

siRNAs. siRNA duplexes targeting various domains of the HAV nonstructural proteins were designed and synthetically prepared as described previously (26). The nucleotide (nt) sequences of the siRNAs were the following (5′ to 3′): 2C-1 (GGUUGAAGUUAAACCUGCUUU, nt 4796 to 4813; accession number M59808 augmented with known 5′- and 3′-terminal bases); 2C-2 (UGAUAUG UUGAAUGUUAAUUU; nt 4838 to 4856); 3A (UGAUAGUGCAGUAGCU GAGUU; nt 5030 to 5048); 3C (UAGAGGUGGAACUUACUAUUU; nt 5480 to 5498); 3D-1 (AGCUGAAAUUGAUCCAAUGUU; nt 6089 to 6107); and 3D-2 (GAAACUUGGCAUGACAGCUUU; nt 7073 to 7091). In addition, the mutated siRNA 2C-1mut containing four nucleotide mutations (shown in bold) was used as a control for target specificity (G**A**UUGAAGU**C**AAACC**A**GC**A** **UU**). All siRNA duplexes contained two uridine residues at the 3′ ends, and their location in the HAV genome is schematically depicted below in Fig. 1. Control siRNAs targeting β-actin or a scrambled sequence were obtained from Ambion.

siRNA transfection. The efficiency of cell transfection was optimized using carboxyfluorescein-labeled negative control siRNA (Ambion). More than 80% of the cells were transfected using 80 pmol of carboxyfluorescein-labeled siRNA per 10^4 cells in a six-well plate at 30 to 40% confluence (not shown). This amount of siRNA was used in all transfection experiments. BS-C-1 and Huh-7 cells were grown to 30 to 40% confluence in antibiotic-free medium in a six-well plate. Eighty picomoles of siRNA in 0.25 ml OptiMEM-1 (Invitrogen) and 4 μl Lipofectamine 2000 (Invitrogen) in 0.25 ml OptiMEM were incubated separately for 5 min at room temperature before incubating them together for 20 min at room temperature. The liposome/siRNA complex was added to the cells previously washed with 1 ml OptiMEM. The cells were incubated at 37°C for 6 h with rocking the plate every 15 min to prevent cell drying. Immediately after siRNA treatment, the cells were either infected with HAV or transfected with synthetic HAV transcripts (see below). Consecutive siRNA transfections, if applied, were performed similarly to single transfection.

HAV infection with viral inoculum (acute infection). The HAV inoculum prepared by multiple passages of HAV (strain 18f) in BS-C-1 cells was used to infect siRNA-transfected BS-C-1 or Huh-7 cells at an MOI of 0.1 $TCID_{50}$/cell. After 3 to 4 h of incubation at 37°C, the inoculum was replaced with antibiotic-free growth medium (DMEM10), which was changed every 4 to 5 days. The cells were harvested at the indicated time points in 0.25 ml 150 mM phosphate-buffered saline, pH 7.5 (PBS) containing 0.05% Tween 20 (PBS-T), and the cell lysate was prepared as described below.

HAV infection with synthetic transcripts. Immediately after the first treatment of Huh-7 cells with siRNAs as described above, 1 μg synthetic HAV RNA produced by T7 in vitro transcription of pT7-18f (strain 18f) (32) was transfected into 10^4 cells (one well of a six-well plate) using 3 μl DMRIE-C as recommended by the manufacturer (Invitrogen). After 6 h, the transfection mixture was replaced by growth medium without antibiotics (DMEM10), and the incubation was continued with medium change every 4 to 5 days. At day 3 to 5 posttransfection (p.t.), cells of two wells were harvested to assay the HAV antigen level and infectivity, while the cells from the other two wells were split 1:4 and transfected again 1 day later with the same siRNAs at a confluence of approximately 30% to 40%. siRNA transfections were repeated three times in total.

siRNA transfection of persistently infected cells (established HAV infection). Persistently infected Huh-7/HAV cells in six-well plates were siRNA transfected as described above. The cells were harvested in duplicate at days 1 and 6 p.t. At day 5 p.t., the cells in two wells were split 1:4. After reaching 30 to 40% confluence (usually the next day), they were used for a second transfection with the same siRNA (day 6). Four days later, the transfected cells of two wells were harvested (day 10), whereas the other two wells were split 1:4 on day 9 p.t. and transfected with siRNA on day 10. The final cell harvest was done on day 14 p.t.

Analysis of cell lysate. After three cycles of freeze-thaw, the cell lysate was clarified by centrifugation and the supernatant was used to analyze HAV antigen, infectivity by end point titration, and β-actin and viral proteins by immunoblotting. The number of HAV genome copies was determined by real-time reverse transcription-PCR (RT-PCR). The nucleotide sequence of the rescued viral genome was determined after RT-PCR amplification of the target region (see below).

HAV antigen detection. The particle-specific enzyme-linked immunosorbent assay with monoclonal anti-HAV antibody 7E7 (Mediagnost, Germany) was applied to detect the HAV antigen (32). Immunoblot analysis of VP1 was performed as described before (32).

End point titration. To determine the HAV infectivity after siRNA treatment, cell lysates were diluted in OptiMEM and 0.25 ml of each dilution was inoculated into 4 wells of Huh-7 cells grown in a 24-well plate. After 3 h of incubation at 37°C, the inoculum was replaced with 0.5 ml of maintenance medium and the incubation was continued with medium change every 5 days. Eleven to 12 days later, the infected cells were washed with 0.5 ml PBS prior to the addition of 0.2 ml PBS-T. The cells were broken up by freeze-thawing directly in the plate, and 0.1 ml of the extract was assayed for HAV antigen (see above). The $TCID_{50}$/ml was calculated according to the Reed-Muench method.

HAV genome quantification. Total RNA was extracted with TRIzol (Invitrogen), and HAV RNA was reverse transcribed at 50°C for 1 h using 2.5 mM oligo$(dT)_{15–18}$ and 10 U/μl SuperScript III (Invitrogen). Real-time PCR with 0.5 μM primers specific for HAV 3C (sense, 5′-ACTTTGGAAATAGCAGGACT GG-3′; antisense, 5′-AGATTGATTCGATGAAACC-3′) was performed by using SYBR Green supermix (Bio-Rad) in a Bio-Rad iCycler. The profile included an incubation at 95°C for 5 min and 35 cycles of 30 s at 94°C, 55°C, and 72°C. The data were normalized to glyceraldehyde-3-phosphate dehydrogenase (GAPDH) gene amplification using the same profile, except for the annealing temperature (62°C instead of 55°C). The following GAPDH-specific primers were used: sense, 5′-AACAGCGACACCCACTCCTC-3′; antisense, 5′-GGAGGGGAGATTCA GTGTGGT-3′. Full-length HAV cDNA was used as the standard for quantitative PCR.

Sequencing of the rescued viral genome. Cytoplasmic RNA was extracted with TRIzol (Invitrogen) from siRNA-treated HAV-infected Huh-7 cells, persistently infected Huh-7/HAV cells, or Huh-7 cells transfected with synthetic HAV RNA, reverse transcribed, and PCR amplified using the C.therm. polymerase one-step RT-PCR system (Roche) and sense and antisense primers targeting genome regions encoding HAV 2C (5′-TGATGGAGTTAAGGACTGCGAGTTTTTC CAACTGGTTA-3′ and 5′-CATTATCATCTGAAATTCCCCGAGACCACAA CTCCATGAATTCAG-3′), 3A (5′-AGAGGGGGAGGAGAGAGCTTAACA TCGATTGCATTG-3′ and 5′-GTCCTGCTATTTCCAAAGTTAACTGAGAT TCTACTGGATCTGCATC-3′), 3C (5′-GATGCAGATCCAGTAGAATCTCA GTTAACTTTGGAAATAGCAGGAC-3′ and 5′-GTAAACTCCACTTTCAT AATTCTCTTACTTTCAATTTTCTTATC-3′), or 3D (5′-GATAAGAAAATT GAAAGTAAGAGAATTATGAAAGTGGAGTTTAC-3′ and 5′-GACTGAA CAAAATAATAGAATTTCTGATAAAACTCATAGCCATGC-3′) according to the manufacturer's protocol. The 2C amplification product was sequenced with the sense primer 5′-ATTAGTTTGCATCATTGATGATATTGGCCAAA ACACAA-3′, for analyzing the sequence of both 2C target regions. For sequencing the 3A and 3C amplification products, the antisense primer 5′-ACACCATG ATATACCCCTTGAGCTGGGATTGGTTCTTCCTC-3′ and sense primer 5′-GT AATATCTCTAAACTGAGGAATTGTAGGAACCTTCATCAG-3′ were used, respectively. The sense 5′-GTTTTAATAGTTTCTCGAGATGTACAGATCGAT AATCTTGATTTGAT-3′ and the antisense 5′-GTATGGAAACCTGGATTC-3′ primers were used to sequence the 3D-1 and 3D-2 target regions in the RT-PCR amplification product of the rescued viruses. Sequencing was performed by the dideoxynucleotide termination method (AGOWA, Berlin, Germany).

Reporter gene expression. HAV and poliovirus replicon RNAs were transcribed with T7 RNA polymerase (RiboMax; Promega) from plasmids pT7-18f–

LUC–A60 (33) and pRLuc181 (kind gift of R. Andino) linearized with AgeI and MluI, respectively. Runoff transcripts were characterized by denaturing 0.8% agarose gel and spectrophotometry before transfection into Huh-7 cells. Luciferase activity was measured as described previously (16).

Preparation of RNAi-resistant genomes. The QuikChange site-directed mutagenesis procedure (Stratagene) was used to insert mutations into the 3D-1 and 3D-2 target sites of the full-length (33) and firefly luciferase-encoding HAV cDNAs. For this, the sense primer 5′-gctatgccctttttctaaAGC**A**GA**G**ATTGATCC AATGgctgtgatgttatctaag-3′ or 5′-caaaaaattgtagatgagtttaaGAA**G**CTTGG**T**ATG ACAGCTacttctgctgacaag-3′ and their complementary oligonucleotides, respectively, were used. The target regions and mutated nucleotides are shown in capital letters and bold, respectively. Before transfer of a PflMI-AatII fragment into dephosphorylated and restricted with the same enzymes pT7–18f–A60 and replicon pT7-18f–LUC–A60 (33), the sequence of a fragment containing a double-mutated 3D-1 region (3.3 kb) was verified (AGOWA, Berlin, Germany). The transfer of the fragment containing a double-mutated 3D-2 region (2.5 kb) into both plasmids was performed in a similar way using XhoI and AatII restriction enzymes. After linearization with AgeI, T7 transcripts of the parental and mutated viral and replicon genomes were generated and analyzed as described earlier (33). Two consecutive transfections of double-mutated full-length and replicon RNAs into siRNA-pretreated Huh-7 cells were done in triplicate and quadruplicate, respectively.

RNA secondary structure prediction. An online siRNA design service (MWG siMAX) was used to anticipate possible genome sites within HAV for effective siRNAs. Possible local secondary structures (optimal energy) for these regions were generated as part of these procedures. The sequence of HAV-18f (accession number M59808) was extended to include known 5′- and 3′-terminal bases and analyzed in its entirety (7,507 bases) for optimal and suboptimal folding patterns, using methods similar to other picornaviruses (44). The P-num (pairing number) values are a standard output for this method and tabulate the relative fidelity with which each base in the optimal fold would choose to maintain that configuration, if offered a defined energy window (+12 kcal) near the optimal (−1,848 kcal). The match value tests the number of times (percent) a base was observed to take its most popular pairing partner in the sampled cohort (100 times) of suboptimal structures within an energy window (+9 kcal) near the optimum.

RESULTS

Recently, we have shown that replication of the HAV replicon encoding the firefly luciferase in place of the viral capsid proteins was efficiently suppressed by siRNAs targeting various domains of the nonstructural proteins or the reporter gene (26, 34). Preliminary data indicated that some of these siRNAs might also silence HAV infection. However, antiviral interference with siRNAs faces major challenges, as this virus replicates slowly and its RNA might outlast the half-life of siRNAs. To advance our understanding of the molecular requirements and genetic consequences of efficient RNAi, HAV replication under various cell culture conditions was tested in the presence of a set of siRNAs that were successfully used to inhibit HAV subgenomic RNA replication (26). The following parameters were analyzed: (i) host cells that distinctively support HAV replication; (ii) various schemes of infection (acute, persistent, or initiated by the HAV RNA transcript); (iii) single or multiple applications of one or more siRNAs; finally, (iv) emergence of escape mutations in the siRNA target region.

Silencing of acute HAV infection. HAV-susceptible BS-C-1 cells were transfected with the synthetic siRNA duplexes 2C-1, 2C-2, 3A, 3C, 3D-1, and 3D-2 targeting the HAV genome at the sites indicated in Fig. 1. Note that target site 2C-1 is located in a stem-loop structure of the computer-folded full-length HAV genome and more exposed than any of the other targets (see below). Immediately after siRNA transfection, the cells were infected with the 18f variant of HAV strain HM175. A scrambled siRNA was used as a negative control (Ambion). To assess suppression of HAV replication, the decrease in viral particle formation and the reduction of viral infectivity were determined by an enzyme-linked immunosorbent assay and by end point titration, respectively. Moderate suppression of viral particle formation was observed 5 and 10 days p.t. (not shown). Depending on the siRNA used, the infectious titer ($TCID_{50}$/ml) decreased by 0.75 to 2.5 orders of magnitude compared to cells treated with control siRNA (data not shown). At day 15 p.t., the suppression levels were less than at earlier time points (maximum, 15% inhibition of particle formation and 0.25 log for infectivity). Possibly due to the short half-life of the transfected siRNAs compared to the slow and asynchronous replication of HAV, crucial RNAi levels were only attained at early stages of infection. Alternatively, the emergence of mutant viruses that had escaped RNAi might be reason for abating RNAi (21). To prevent the emergence of siRNA-resistant mutants, we treated HAV-infected cells with a mixture of two siRNAs. Compared to the effect of a single siRNA, two siRNAs combined induced a more sustained suppression, albeit the effect was not additive (not shown). At 10 and 15 days p.t., inhibition of viral particle formation and infectivity was twice as high when two RNAs were used in combination, implying that besides the short half-life of the siRNA duplexes, the emergence of viral escape mutants may limit the efficiency of RNAi (see below).

HAV replication is less efficient in BS-C-1 cells than in liver cells, which are the natural host for HAV replication in vivo and produce larger amounts of infectious virus (35, 47) or viral replicon (16, 57). To test whether the extent of RNAi depended on the host cell line and the rate of viral replication, the human hepatoma cell line Huh-7 was transfected with the same set of siRNAs and infected with HAV as described above. In contrast to BS-C-1 cells, in Huh-7 cells HAV infection was inhibited in a sustained manner (Fig. 2A, B, and C). A $10^{4.7}$-fold suppression of infectivity was observed 4 days p.t. (Fig. 2A), with the tendency to decrease over time (2.6 orders of magnitude at day 8 p.t. [Fig. 2B] and 1.6 log at day 12 p.t. [Fig. 2C]). All HAV-specific siRNAs suppressed HAV replication to almost the same extent ($TCID_{50}$/ml values varied maximally by ±0.5 log (Fig. 2A, B, and C), which was confirmed after quantitative analysis of the viral structural protein VP1 by immunoblotting (data not shown). As mentioned above and further analyzed below, the loss of specific suppression of HAV infection at late time points might reflect the emergence of mutant viruses escaping RNAi.

To directly measure the loss of viral genomes by RNAi, the viral genome copy number was determined by real-time RT-PCR in siRNA-treated and HAV-infected Huh-7 cells 4 and 12 days p.t. The genome equivalent/infectious particle ratio was 1×10^2 in the case of cells treated for 4 days with control siRNA ($1 \times 10^{8.57}$ physical genomes to $1 \times 10^{6.6}$ of infectious viral particles), whereas the ratio was approximately $10^{4.0}$ in HAV siRNA-treated cells ($1 \times 10^{6.2}$ genome copies per $1 \times 10^{2.2}$ infectious particles) (Fig. 2A). The reduction in genome number was clearly less pronounced than the loss of infectivity as detected by end point titration (Fig. 2A, B, and C), implying that degradation of viral RNA mediated by specific siRNAs is incomplete. Apparently, partially degraded yet noninfectious genomes were still detected by real-time RT-PCR. At a later

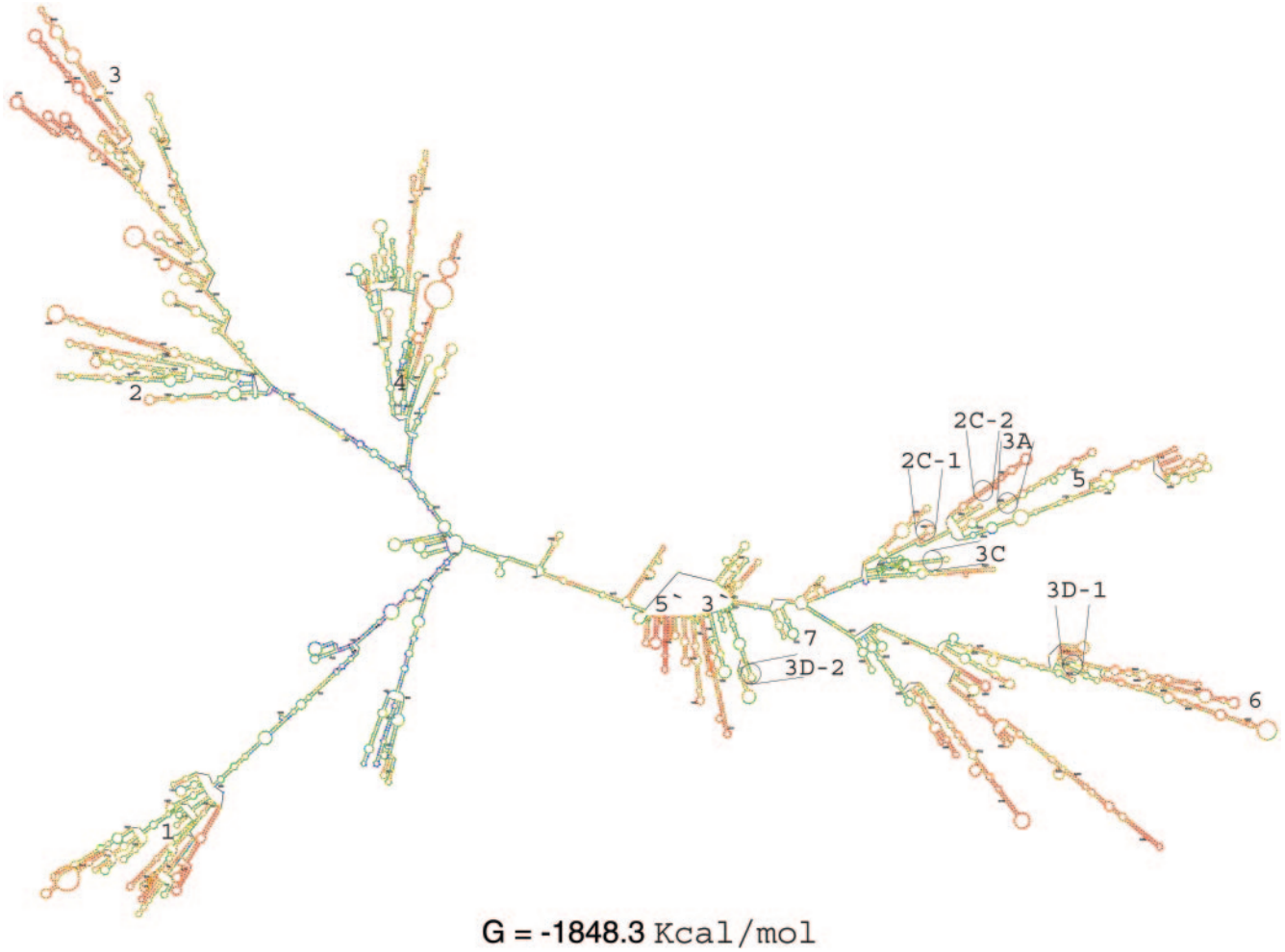

FIG. 1. Approximate location of the siRNA target sequences within an optimal structure of the HAV genome (strain 18f). Sequence M59808 was augmented with known 5′- and 3′-terminal bases and then analyzed by mFold. Base numbers (shown in blue) are in increments of 1,000. Each base in the minimum free energy structure is color coded on a sliding scale, according to its pairing number (P-num), with red, orange, yellow, green, blue, and violet indicating successively higher frequencies of potential alternative configurations within an energy window of +12 kcal from the optimal (44).

time point, the difference in genome number in cells treated with HAV-specific and unspecific siRNAs was marginal.

In order to assess whether a short-term RNAi effect can be prolonged and also to prevent the escape of RNAi-resistant viral mutants, different siRNAs were consecutively transfected into HAV-infected cells. Acutely infected Huh-7 cells were transfected on days 0, 2, 5, and 8 with various siRNAs as indicated (Fig. 2D), and the infectious titer was determined 12 days postinfection. Viral replication was substantially more suppressed after consecutive siRNAs applications (titer reduction by 3.7 log [Fig. 2D] compared to 1.6 log for single application [Fig. 2C]). A similar enhancement of RNAi by consecutive siRNA applications was also obvious in HAV-infected BS-C-1 cells. At day 15 p.t., the acute HAV infection as judged by infectivity titer was 37 times more efficiently suppressed than that after a single siRNA transfection (not shown). The reduction of the infectious titer was in good agreement with the loss of HAV genome copies detected by real-time RT-PCR, indicating that siRNA genome degradation was more efficient after repeated siRNA treatments compared to a single transfection (not shown). Taken together, the results suggest that HAV RNAi was sustained after consecutive siRNA transfection and depended on the viral replication rate, which was influenced by the host cells (35). Substantially stronger inhibition of the acute HAV infection was achieved in human hepatoma cells than in BS-C-1 cells, and viral replication was significantly more suppressed when siRNAs targeting different HAV genomic regions were consecutively applied.

RNAi targeting the established HAV infection. The data obtained with Huh-7 cells (Fig. 2) clearly indicated that siRNAs delivered into the cells at the same time as the viral inoculum (acute infection) can efficiently suppress HAV replication and may thus be of therapeutic use. However, in order to treat severe cases of acute hepatitis A and possibly fulminant liver failure (52), an ongoing HAV infection has to be suppressed. To address this issue in a model system, a persistent HAV infection in hepatoma cells (Huh-7/HAV) was established and its suppression by RNAi was studied. Since in

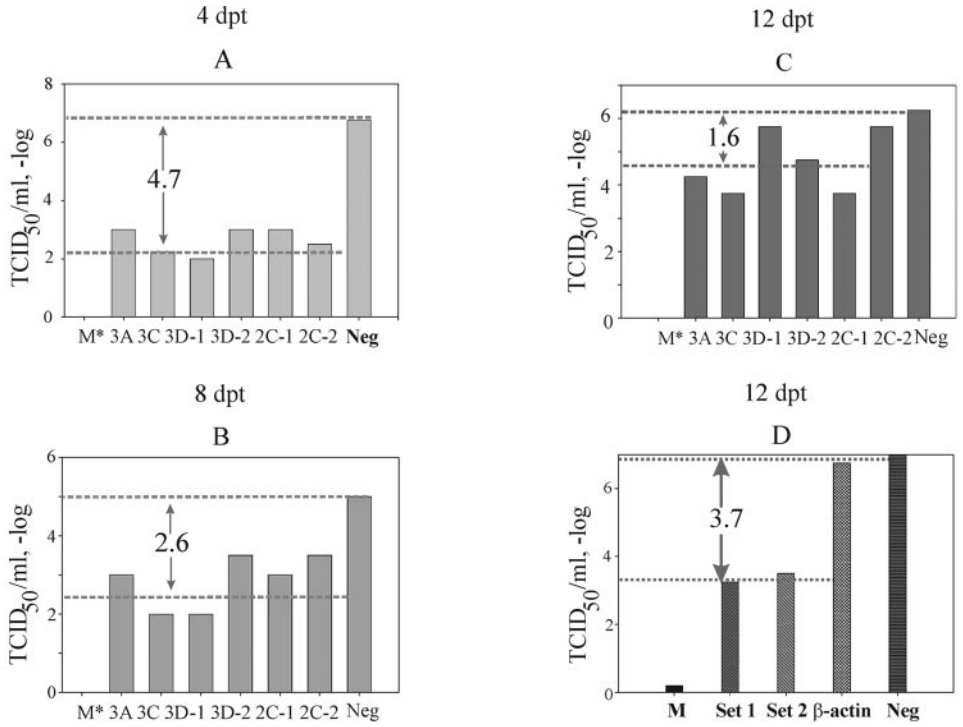

FIG. 2. Suppression of HAV infectivity after single (A, B, and C) and multiple (D) applications of siRNAs in acutely infected Huh-7 cells. Days posttransfection (dpt) are indicated above the diagrams. Individual siRNA duplexes used for silencing are marked below the columns. Neg, transfection with scrambled siRNA; M*, mock-transfected and uninfected cells. The lower dotted lines indicate the approximate mean values of the infectivity after treatment of the HAV infection with indicated HAV-specific siRNAs. The differenced in infectious titer of cells treated with negative control siRNA (Neg or β-actin; upper dotted lines) and HAV-specific siRNAs (lower dotted lines) are shown by numbers between arrows. In panel D, the following single siRNAs (set 1) were sequentially transfected in HAV-infected cells on days 0, 2, 5, and 8: 3C, 3A, 2C-1, and 2C-2, respectively. In set 2, siRNAs 2C-1, 3D-1, 3D-1, and 3D-2 were used at the same days in a parallel experiment. At day 12 posttransfection/infection, the cells were harvested and the HAV infectious titer was determined. The values represent the mean titers of two independent experiments.

persistently infected cells viral genome replication is highly retarded with only a small proportion of the genomes replicating, we aimed to stimulate viral replication. To this end, persistently infected Huh-7/HAV cells were induced to divide by splitting them 1 day prior to siRNA treatment, as we had recently shown that viral replication is enhanced in actively dividing cells (35). Moreover, to enhance the silencing efficacy, applications with the same siRNA were repeated. The data presented in Fig. 3A clearly show that siRNA 2C-1 efficiently suppressed the formation of viral particles, in particular after the second and third siRNA applications. In parallel, the infectivity titer decreased after each application of siRNA 2C-1, resulting in a 3-log reduction after three consecutive applications (Fig. 3B).

A similar loss of HAV antigen was observed after multiple applications of siRNA 3C (Fig. 3A). However, this effect seemed to be mostly due to stress-related cell death upon repeated siRNA transfections. Weak or no suppression of the HAV antigen (30% to 40%) was observed after transfection of siRNAs 2C-2 and 3A. Intriguingly, after three applications of siRNA 2C-2, the infectious titer increased compared to transfection with negative control siRNA (Fig. 3B). The two first applications of siRNAs 3D-1 and 3D-2 suppressed viral particle formation to approximately 30% to 50%. However, the initial HAV antigen level (Fig. 3A) and infectivity (not shown) were almost restored after an additional siRNA treatment. While similar infectious titers (10^7 $TCID_{50}$/ml) were detectable in acutely and persistently infected cells, the established HAV infection was much less suppressed than the acute infection (Fig. 2), implying that a large proportion of the viral genomes in persistently infected cells were inaccessible to the RNAi machinery. Although not directly proven here, observations of ours and another group suggest that most HAV genomes in persistently infected cells are packaged and only a minor fraction of all potentially infectious genomes is actively replicating and accessible to gene silencing (reference 2 and unpublished observation). The data may also imply that RNAi-resistant viral mutants might have emerged from the viral quasispecies genome present in persistently infected cells.

To determine whether the appearance of siRNA-resistant mutants after multiple siRNA applications was the cause for the increase in viral antigen level and infectivity (Fig. 3A and B), total RNA was isolated from the lysates of infected and siRNA-treated cells (Fig. 3A) and the viral genomes were sequenced after RT-PCR amplification of the target domain. As expected, viral genomes that had resisted the treatment with siRNA 3D-1 and 3D-2 carried mutations in the target sequences (Fig. 4, bottom row, middle and right panels). At the indicated time point, a mixture of two nucleotides was found at positions 4 and 7 of target 3D-1 and at position 4 of target 3D-2, suggesting the selection of RNAi-resistant sequences from the viral quasispecies. As these nucleotide exchanges

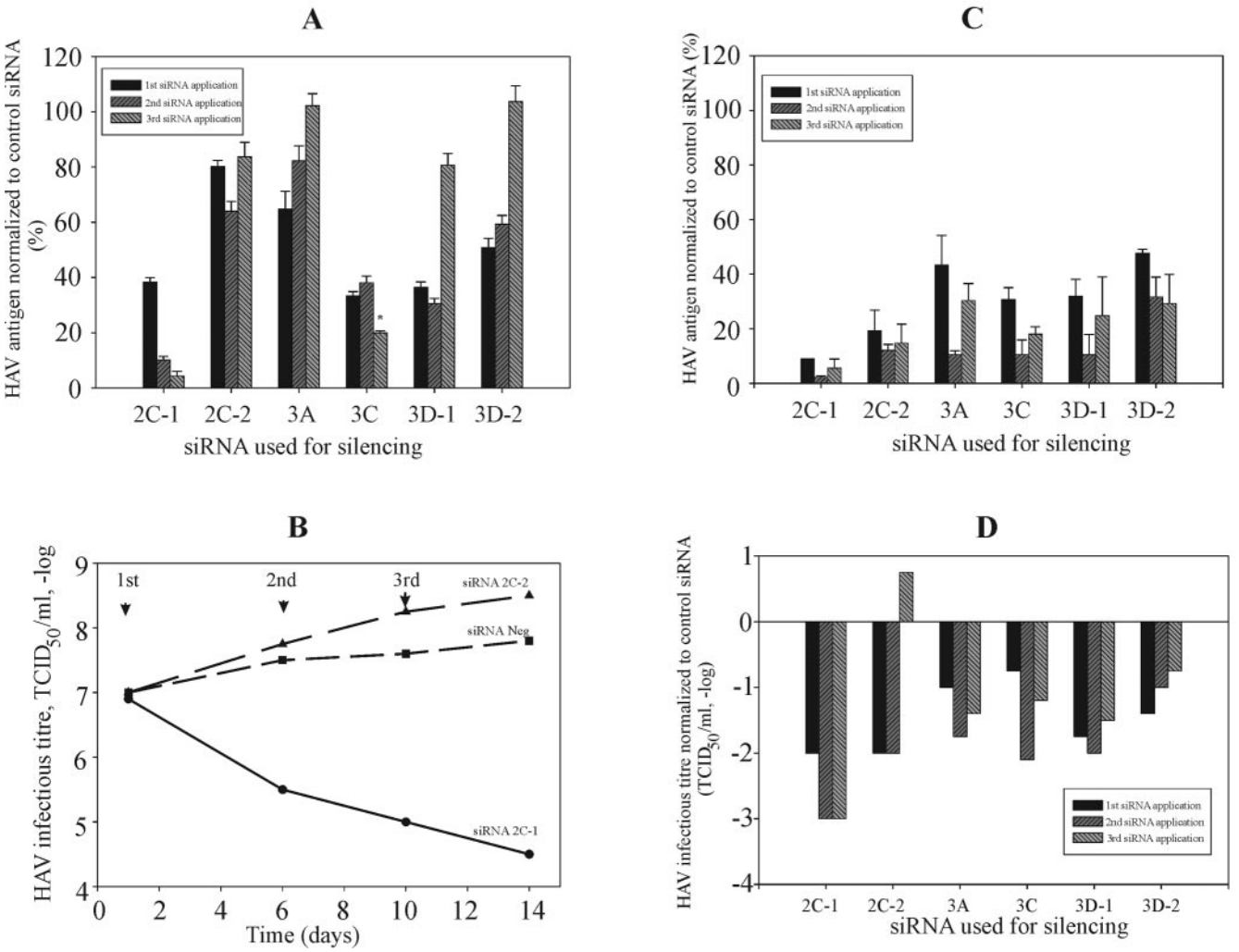

FIG. 3. siRNA-mediated suppression of the established HAV infection (A and B) and infection initiated by synthetic HAV transcript (C and D). (A and C) Relative inhibition of the viral antigen after three consecutive siRNA applications. HAV antigen that accumulated in cells that were treated with the control siRNA was set at 100%. The mean values and standard deviations of duplicate samples are shown as bars and lines, respectively. Note that in the case of the established HAV infection (A), after the third treatment with siRNAs 3D-1 and 3D-2 the original antigen level was restored. The asterisk in panel A denotes nonspecific cell degeneration by siRNA 3C. (B) Suppression of the infectious titer in an established infection by siRNA 2C-1 (dots) and siRNA 2C-2 (triangles). Arrows indicate the siRNA applications. The infectivity data in cells treated with control siRNA are shown for comparison (squares). (D) siRNA-mediated inhibition of the HAV infectivity originated from synthetic viral RNA. The inhibition was calculated after dividing the infectious titer of control siRNA-treated cells by the titer of HAV siRNA-treated cells.

were in the wobble position of the codons, none of the mutations resulted in an altered amino acid residue. Interestingly, the C-to-U substitution causing a G-U mismatch in the central position (11th nt) of the 3D-2 target site (bottom row, right panel) was complete and similar to that described for poliovirus (21).

Nucleotide sequence determination of the 2C-2 target region revealed that positions 11 and 17 were partially mutated, resulting in a change from amino acid residue asparagine (N) to aspartic acid (D) in both positions (Fig. 4, bottom row, left panel). No nucleotide changes were found in the 3A and 3C target regions of the rescued viruses (not shown). As overall suppression by siRNAs 3A and 3C was either low or nonspecific, this suggests that these targets were mostly inaccessible for RNAi. Finally, sequence analysis of the virus present in low amounts after the third treatment with siRNA 2C-1 revealed no changes (not shown). Taken together, the analysis of the viral genomes rescued after siRNA treatments of HAV-infected cells revealed that the RNAi efficacy significantly depended on the target region. Whereas RNAi-resistant escape mutants were found for targets 2C-2, 3D-1, and 3D-2, no specific effect was achieved with siRNAs 3A and 3C and a strong silencing effect with siRNA targeting 2C-1 was observed. As the target of RNAi was the quasispecies genome of the actively replicating virus, it is most likely that these RNAi-resistant variants were already present in the quasispecies populations and that their replication was favored under the siRNA-specific selection pressure (see also reference 54). However, the possibility cannot be excluded that the viral genome had mutated in the target region under the siRNA pressure.

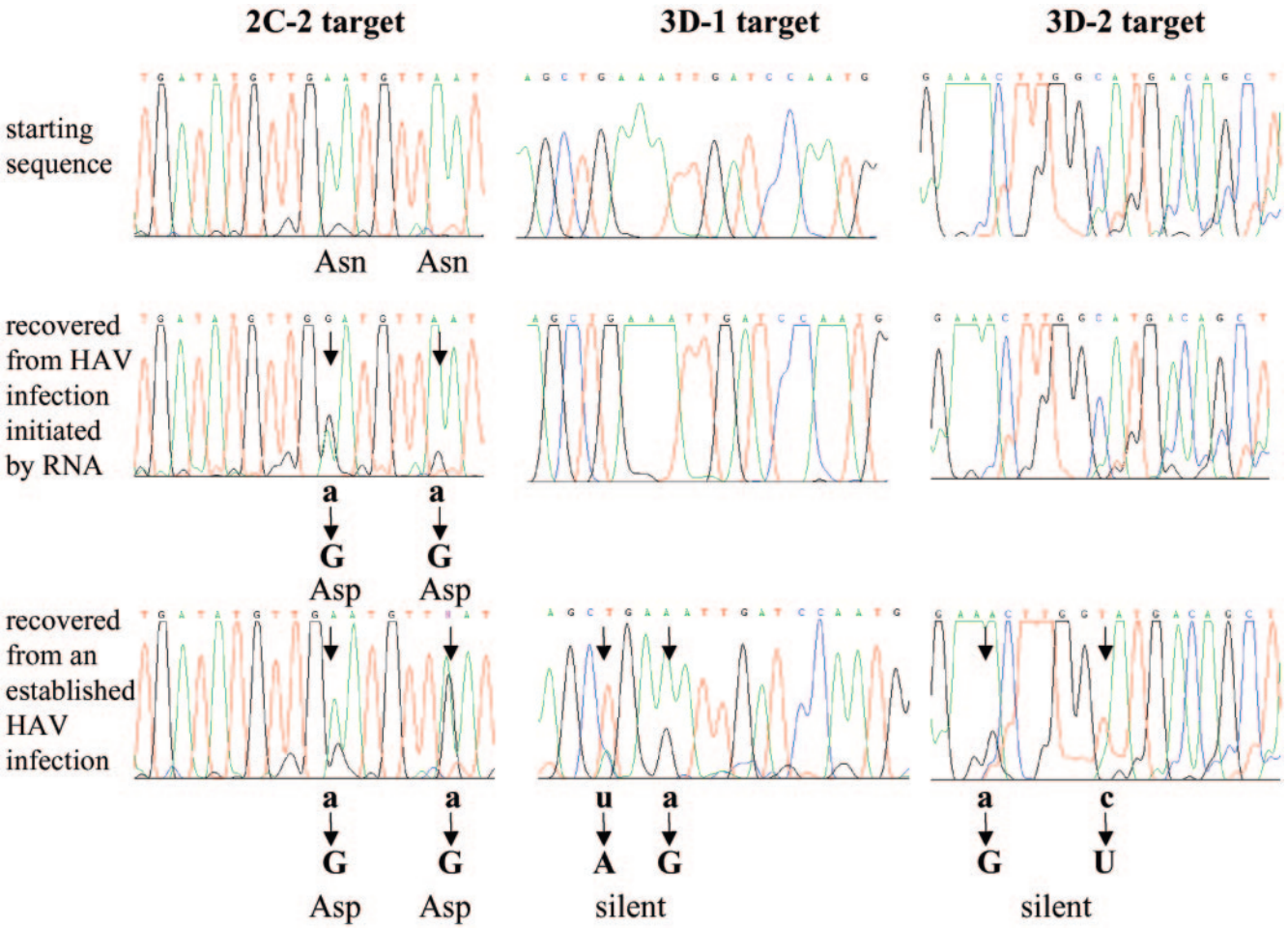

FIG. 4. Population sequencing of viral genomes in the target regions of siRNAs 2C-2, 3D-1, and 3D-2 after three treatments with the corresponding siRNA duplexes. The top sequences represents the viral or transcript genome used for infection (upper panels). The sequences in the middle were recovered from the viral RNA of siRNA-treated cells infected by synthetic RNA, whereas the sequences below were recovered from siRNA-treated cells with an established HAV infection. The mutations in 3D-1 and 3D-2 are silent. The parental and mutated nucleotides are shown in small and capital letters, respectively. Two A-to-G mutations in the 2C-2 target sequence result in Asn-to-Asp changes, shown below the sequence chromatograms. Arrows in the chromatogram mark the altered nucleotides.

RNAi targeting HAV infection initiated by synthetic RNA. To distinguish between these two possibilities, in the next experiment viral replication was initiated by infectious synthetic transcripts that encode perfectly matching target sequences. Huh-7 cells were simultaneously transfected with infectious transcripts and the various siRNAs. To ensure sustained silencing, additional siRNA transfections followed, as described above for the persistently infected cells (Fig. 3C). siRNA treatment of HAV RNA-transfected cells inhibited the viral particle formation more profoundly than that of the ongoing HAV infection in persistently infected cells (compare Fig. 3A and C), supporting our earlier observation that a large proportion of the viral genomes in persistently infected cells is protected from RNAi. Again, siRNA 2C-1 was found to be the most efficient silencer (92% inhibition), whereas siRNAs targeting 2C-2, 3A, 3C, 3D-1, and 3D-2 domains were less effective after the first treatment (80%, 56%, 79%, 78%, and 52% inhibition, respectively) (Fig. 3C). Compared to acutely (Fig. 2A) and persistently (Fig. 3A) infected cells, a similar number of infectious viral genomes was present in RNA-transfected cells as the absolute titer reached 10^7 $TCID_{50}$/ml at 4 days p.t. The second application of siRNAs enhanced the suppression of the HAV antigen (Fig. 3C). Intriguingly, after the third siRNA application, the level of the HAV suppression was no longer enhanced but was slightly decreased. The loss in HAV antigen levels roughly correlated with the drop in the infectious titer determined after the various siRNA treatments (Fig. 3C and D). Compared to the $TCID_{50}$/ml values obtained with the control siRNA, three applications of siRNA 2C-1 decreased the infectious titer by 3 orders of magnitude. For all other siRNAs, except 2C-2, the infectious titer values were below those of the control siRNA by 0.5 to 1.5 orders of magnitude. Intriguingly, the infectious titer for siRNA 2C-2-treated cells was reproducibly higher than that of the control siRNA (0.5 to 1.0 orders of magnitude) (Fig. 3D). When RNAi of the ongoing infection (Fig. 3A and B) was directly compared with the silencing of HAV replication initiated by synthetic transcripts (Fig. 3C and D) or the viral inoculum (Fig. 2), it was obvious that a higher silencing effect was achieved under the latter conditions. Whereas in the ongoing HAV infection the sup-

pression of viral particle formation after one siRNA application was maximally 70%, it was up to 95% in infections initiated by synthetic HAV RNA and similar to that of the acute infection (compare Fig. 3A and C and Fig. 2). Most likely, the limited RNAi effect on an ongoing HAV infection was due to the inaccessibility of a substantial portion of the viral genomes that were packaged.

To examine whether RNAi-resistant viral variants had evolved under the infection and selection conditions described for Fig. 3, the total RNA of the HAV-expressing cells treated three times with siRNA was used for sequence determination as described above. In contrast to RNAi of the established HAV infection (Fig. 4, bottom row, middle and right panels), neither of the viral genomes derived from synthetic RNA and replicating in the presence of siRNAs 3D-1 or 3D-2 had nucleotide changes (Fig. 4, middle row, middle and right panels). Interestingly, a similar difference between resistant mutants emerging from synthetic transcripts or established replications was recently described for HCV (56). Moreover, the genomes replicating in the presence of siRNAs 2C-1, 3A, and 3C were unchanged under the selective pressure used (not shown). However, similar to the siRNA 2C-2-mediated silencing of the ongoing infection (bottom row, left panel), the virus that emerged from synthetic transcripts carried mutations at the 2C-2 target positions A11G and A17G (middle row, left panel). These mutations resulted in an amino acid change from Asn to Asp. Under all experimental conditions used, the A11G and A17G mutations in target 2C-2 were always and repeatedly found in the background of the parental sequence. Clonal isolation of the rescued virus will be necessary to determine whether both mutations occurred in one genome and whether the wild-type virus and its nonstructural protein 2C is required (as a *trans*-acting factor) for replication of the mutated genome. Interestingly, the infectious titer of the virus evading three siRNA 2C-2 applications was always higher than that of the negative control (Fig. 3B and D). This implies that a more efficiently replicating virus with amino acid replacements in 2C (Asn to Asp) had evolved under siRNA 2C-2 suppression. This observation was confirmed by HAV genome quantification using real-time RT-PCR. One hundred times more genome copies were found after the third siRNA 2C-2 treatment compared to that of the scrambled siRNA (not shown). Collectively, the data presented here for the slowly replicating HAV suggest that the fraction of replicating genomes among the viral RNA and the rate of RNA synthesis and thus of mutation are major determinants for the efficiency of RNAi and the emergence of siRNA-resistant escape mutants.

To further demonstrate that the observed RNAi was HAV specific, the suppressive effect of selected siRNAs was tested on the poliovirus replicon and different HAV strains. Luciferase expression of the poliovirus replicon was unaffected in the presence of 2C-1, 2C-1mut, and scrambled control siRNAs. In contrast, the luciferase activity of the HAV replicon (33) was significantly inhibited by siRNA 2C-1 (73.7% inhibition), but not by 2C-1mut (0.6% inhibition). The sequence specificity was further confirmed by comparing the suppressive effect on two HAV strains differing in the 2C-1 target sequence. siRNA 2C-1mut was unable to silence the replication of HAV strain 18f (0.5% inhibition) but efficiently suppressed the replication of the HAV strain (accession number D00924), whose target sequence was identical to the sequence of siRNA 2C-1mut (99.93% of inhibition).

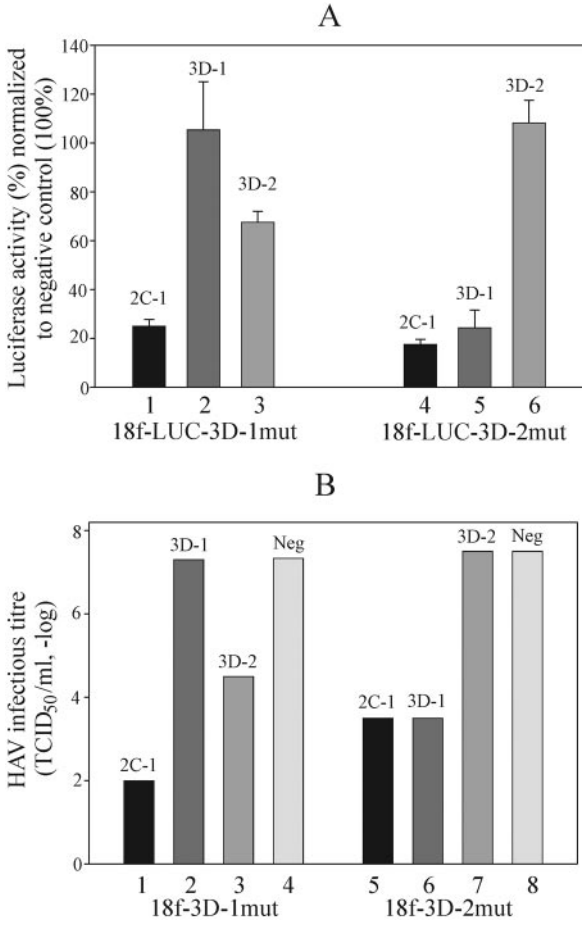

FIG. 5. RNAi resistance of escaping HAV genomes. A. Replicon RNA encoding the mutated target regions 3D-1 (bars 1 to 3) or 3D-2 (bars 4 to 6) was transfected in triplicate into Huh-7 cells pretreated with siRNA 2C-1 (bars 1 and 4), 3D-1 (bars 2 and 5), 3D-2 (bars 3 and 6), or siRNA Neg (used for normalization in panel A). Luciferase activity was measured 24 h p.t. and normalized (percent) to negative control siRNA (100%). B. Full-length HAV RNA transcripts encoding the mutated 3D-1 (bars 1 to 4) or 3D-2 (bars 5 to 8) target regions were transfected into cells that were pretreated with siRNA 2C-1 (bars 1 and 5), 3D-1 (bars 2 and 6), 3D-2 (bars 3 and 7), or siRNA Neg (bars 4 and 8). The infectious titer ($TCID_{50}$/ml) was determined 5 days after a second siRNA application. The middle values of two independent experiments are presented. For the sequences of 3D-1mut and 3D-2mut, see Materials and Methods.

RNAi resistance of escaping viruses. To assess whether the viruses that had escaped RNAi were indeed resistant to siRNA treatment, viral variants (18f-3D-1mut and 18f-3D-2mut) that carried two nucleotide exchanges in the target regions 3D-1 and 3D-2, respectively, were generated by in situ mutagenesis (Fig. 5B). Besides the full-length viral genome, the same mutations were also inserted into the firefly luciferase-encoding replicon, resulting in 18f-LUC-3D-1mut and 18f-LUC-3D-2mut (Fig. 5A). After generation of in vitro transcripts, replication of the mutated genomes was tested for their sensitivity towards both siRNAs 3D-1 and 3D-2. As expected, 18f-LUC-3D-1mut and 18f-LUC-3D-2mut were resistant to siRNA 3D-1 and

3D-2, respectively (Fig. 5A, bars 2 and 6), and sensitive to 2C-1 (bars 1 and 4). In line with previously reported data (Fig. 3A and C) (26), the silence potency of siRNA 3D-2 (bar 3) was weak compared to that of siRNA 3D-1 (bar 5). Using the mutated full-length HAV genomes as targets for RNAi, the siRNA specificity was confirmed (Fig. 5B). The infectious titers of the 18f-3D-1mut and 18f-3D-2mut genomes in the presence of the respective siRNAs were similar to those of the negative controls (bars 2, 4, 7, and 8). Conversely, siRNA 3D-1 only suppressed the infectivity of 18f-3D-2mut (bar 6) without affecting 18f-3D-1mut (bar 2), whereas siRNA 3D-2 inhibited the infectivity of 18f-3D-1mut (bar 3) but not of 18f-3D-2mut (bar 7). Again, siRNA 2C-1 showed extensive inhibition of the HAV infection initiated by synthetic RNA transcripts mutated in the 3D target sites (bars 1 and 5). These data unambiguously confirm the sequence-specific effect of RNAi and suggest that consecutive siRNA applications (Fig. 3A) select mutants that either preexisted in the viral quasispecies genome or were generated during genome replication.

DISCUSSION

Rapidly progressing antiviral strategies based upon RNAi, which down-regulate virus replication by degrading the viral genome, appear highly promising and offer an alternative approach to conventional antiviral therapy. The genomes of RNA viruses function as both translation and replication templates, which makes them an attractive target for siRNAs. However, RNAi is faced with several challenges that must be overcome to realize its promises as an antiviral strategy. Persistently and asynchronously replicating viruses, such as HAV, may present an additional challenge to RNAi, as the siRNA half-life might unfavorably compete with the accessibility of the target site. In addition, the packaged viral genome residing in persistently infected cells efficiently resists RNAi. In fact, the highly efficient sequestration of newly synthesized HAV RNA into virions (2) has been postulated as a way to reduce the viral replication rate and seems to protect a large proportion of viral RNA from silencing. For the interpretation of the data presented here, it has to be kept in mind that identification of RNAi in HAV-infected cells requires multiple cycles due to the virus' slow and asynchronous replication, whereas in poliovirus-infected cells the silencing effect was detected after a single cycle (19, 20).

In the experiments described here, it was striking that the extent of the RNAi effect produced by the same amount of siRNA varied among the cell types used and the type of viral infection. In contrast to Huh-7 cells, HAV infection was weakly silenced in BS-C-1 cells, which support HAV replication less efficiently. In spite of the same overall infectivity present at a given time point (10^7 $TCID_{50}$, 4 days postinfection), we observed that silencing of an ongoing (established) infection was less efficient (up to 3 orders of magnitude) (Fig. 3B) than that of acutely infected Huh-7 cells (4.7 log suppression) (Fig. 2A). This might directly reflect the proportion of accessible target RNA in the background of inaccessible packaged genomes whose infectious nature is still detectable in the subsequent virus titration. Diverse compartmentalization might also explain inaccessibility of the RNA target. The inherent resistance of the hepatitis C or the West Nile virus genome to siRNA treatment was assumed to be due to the location of their replicative form in membranous compartments that are not exposed to the cytoplasmic RNAi machinery (17, 56). Similarly, picornaviruses have been shown to replicate in virus-induced vesicles (10). It can also not be excluded that a substantial proportion of the transfected siRNAs was sequestered by noninfectious transcripts, thus reducing the specific RNAi effect when infection was initiated by a full-length HAV RNA transcript compared to the acute infection (compare Fig. 3D with 2A). A similar dependence of the RNAi effect on the MOI was recently noticed for poliovirus (21).

Even though sophisticated algorithms for the design of siRNAs have been applied, it is often noticed that siRNAs are inefficient in silencing (13, 24, 28, 39). We therefore tested six different siRNAs that are unique to HAV. These siRNAs had been shown to efficiently suppress the replication of the HAV replicon without inducing the double-stranded RNA-activated protein kinase response (26). Interestingly, HAV itself was reported to inhibit cellular antiviral defense mechanisms induced by double-stranded RNA (6). Although all siRNAs were almost equally suppressive in acutely infected cells (Fig. 2 and data not shown), discernible effects were noticed when larger concentrations of viral or replicon target RNA were present owing to different infection schemes. siRNA 2C-1 was found to be most effective, resulting in sustained suppression of an established HAV infection without the emergence of siRNA-resistant mutants. Under the selective pressure of multiple transfections of the siRNAs 2C-2, 3D-1, and 3D-2, viral escape mutants emerged, whereas siRNAs 3A and 3C were grossly inefficient or blocked viral replication in an unspecific way.

We show here that the selection of RNAi-resistant escape mutants was significantly enhanced in an established viral infection compared to an infection initiated by RNA transcripts that encode perfectly matching target regions (Fig. 3). This finding directly supports the notion of the viral quasispecies nature present in an established infection. As an unambiguous prove for the escape mutants' ability to indeed resist RNAi, we showed that replication of full-length or luciferase-encoding HAV RNAs that carried mutations in the 3D-1 or 3D-2 targets were completely resistant to silencing by the original siRNAs (Fig. 5). These experiments emphasize the strict sequence specificity of RNAi. On a broader context, the RNAi specificity was further confirmed by the resistance of the poliovirus replicon to HAV-specific siRNAs.

A number of reasons have been put forward to explain the lack of silencing by siRNAs. They include protein binding (25) as well as secondary and tertiary local structures of the RNA target site that may affect the accessibility of siRNAs (5, 29, 38, 42, 43, 46, 53). When the local RNA folding of the effective and noneffective siRNA-targeted HAV regions was compared at the level of the complete HAV genome (strain 18f), distinct folding patterns were obvious (Fig. 6). The center of siRNAs 2C-1 and 3D-2 targeted a terminal loop. The target regions of the other siRNAs (2C-2, 3A, 3C, and 3D-1) covered internal helices or stacked helical motifs. In addition, prediction of each target's average "match value," a parameter recording the frequency with which particular base pairs were observed in a cohort of suboptimal structures, implied subtle differences in the pairing stabilities of the targeted regions (A. Palmenberg, unpublished observation). By this criterion, targets 3A and 3C

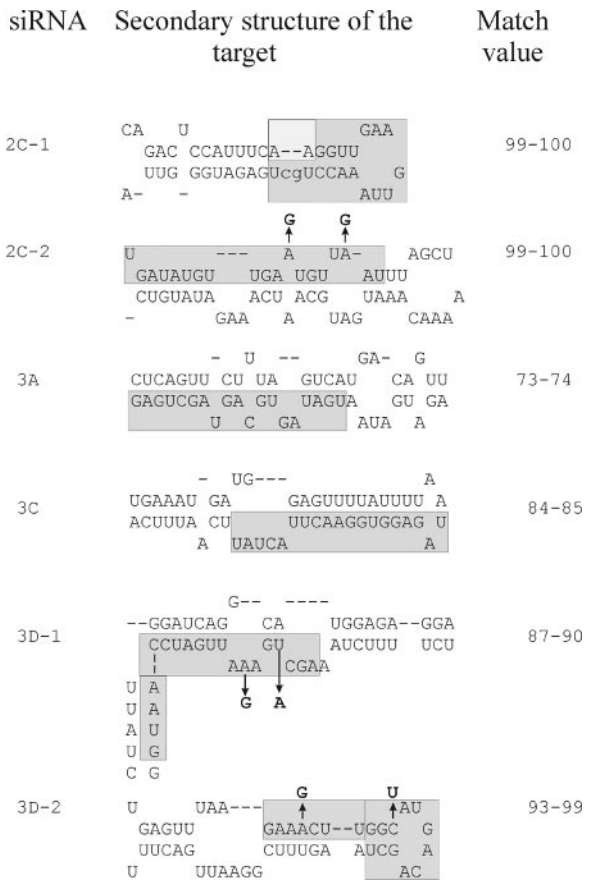

FIG. 6. Computer-predicted secondary structures of the target regions (shown in gray) and match values (range of values for each base in the gray region). The sequence mutations rescued after three siRNA treatments (shown in Fig. 4) are indicated by arrows. The unpaired nucleotides shown in lowercase in 2C-1 (cg) are complementary to a distant region (not shown).

had lower frequencies (73 and 85, respectively) and were less stable or had more alternative potential configurations than the other targets (90 to 100).

Among all HAV targets tested here, 2C-1 with a high match value (99 to 100) was unique in that its local secondary structure was reproducibly stable in the context of the full-length HAV genome (Fig. 6). The other special feature of this target is its large single-stranded loop (6 nucleotides) located in the central region, which is known to be very sensitive for cleavage or mutation (21, 23, 49). Interestingly, no escape virus emerged under the siRNA 2C-1 selection pressure, implying that this target sequence is genetically stable. However, based on the alignment of the 2C-1 target region with some 30-nucleotide sequences deposited in the database, a substantial covariance is found, allowing, for example, a C or a G residue in some target positions. It is highly intriguing that neither of these residues was found in the sequences of the viral genomes selected under the siRNA 2C-1 suppression, implying that the rules governing the RNAi-mediated mutations and spontaneous mutations in natural strains are different.

In contrast to 2C-1, the 3′ half of the 3D-2 target sequence formed a hairpin structure (Fig. 6). Although no 3D-2 target mutations were detected when HAV infection was initiated by RNA transcripts (Fig. 4, right middle panel), mutated target sequences obviously preexisted in the quasispecies genome of the viral inoculum that resisted the siRNA 3D-2 selection pressure (Fig. 4, lower right panel). The mutated 3D-2 target sequence likely folds into a more stable structure than the parental sequence and thus resisted siRNA-mediated degradation. The selection of a more stable secondary and siRNA-resistant structure was recently described for the HIV Nef siRNA-target interaction (55). All other target sequences (2C-2, 3A, 3C, and 3D-1) were found to be part of a double-stranded structure when the full-length HAV genome was computer folded (Fig. 6). Overall, further analyses of the target's secondary structures will be required to better understand their impact for RNAi.

Two types of mismatches were found to be sufficient for the virus to escape interference. In addition to the G-U mismatches in the center of siRNAs 3D-2 and 3D-1, an upstream-located A-A mismatch was identified in the genome of the siRNA 3D-1 escape mutants. This mismatch might be necessary to enhance the escaping ability of the G-U mismatch located in the central region (Fig. 4). Previously, it was observed that if the formation of a duplex with the target sequence required a G-U base pairing, the siRNA failed to efficiently suppress the target sequence (58). In line with our data demonstrating that the centrally located G-U mismatch is sufficient for HAV to escape siRNA suppression (Fig. 4, lower row, right panel), the inability of the G-U base pairs to participate in target recognition during RNAi was recently confirmed by the characterization of poliovirus mutants escaping siRNA inhibition (21).

The viral escape mutant(s) that carried one or two amino acid changes and emerged after multiple siRNA 2C-2 applications was interesting, as it showed reproducibly higher infectious titers (Fig. 3B and D). One or two amino acid changes (Asn to Asp) in the central region and/or close to the 3′ end of the target (Fig. 4, left panels) alone or in combination seem to enhance the viral replication rate. It is noteworthy that these mutations have not been described in the database, yet other sites in the HAV 2C region were previously shown to be responsible for HAV adaptation and efficient growth in cell culture (11, 12). Further experiments are required to elucidate the functional role of the escape mutations in protein 2C for HAV replication in cell culture. In this context the recently described *trans*-dominant effects of mutated viral genomes on the replication of wild-type virus and the concept of the viral quasispecies as a group of interactive variants might be considered for the enhanced replication of a mixture of 2C-2 mutants (8, 54).

A major goal of this study was the identification of an siRNA that could efficiently suppress an active and ongoing HAV infection in a sequence-specific manner. Based on the results reported here, siRNA 2C-1 is a most promising candidate for future therapeutic application to cure severe or fulminant cases of hepatitis A.

ACKNOWLEDGMENTS

We thank B. Andresen, M. Fischer, and F. Horenkamp for excellent technical assistance.

This work was supported by a grant (SFB 367, project B7) from the Deutsche Forschungsgemeinschaft. This work was partially supported

by a Grant-in-aid for Scientific Research from the Ministry of Education, Culture, Sports, Science and Technology, Japan.

REFERENCES

1. **Ahn, J., E. S. Jun, H. S. Lee, S. Y. Yoon, D. H. Kim, H., C-H. Joo, Y. K. Kim, and H. Lee.** 2005. A small interfering RNA targeting coxsackievirus B3 protects permissive HeLa cells from viral challenge. J. Virol. **79:**8620–8624.
2. **Anderson, D. A., B. C. Ross, and S. A. Locarnini.** 1988. Restricted replication of hepatitis A virus in cell culture: encapsidation of viral RNA depletes the pool of RNA available for replication. J. Virol. **62:**4201–4206.
3. **Andre, F., P. Van Damme, A. Safary, and J. Banaivala.** 2002. Inactivated hepatitis A vaccine: immunogenicity, efficacy, safety and review of official recommendations for use. Expert Rev. Vaccines **1:**9–23.
4. **Arbuthnot, P., S. Carmona, and A. Ely.** 2005. Exploiting the RNA interference pathway to counter hepatitis B virus replication. Liver Int. **25:**9–15.
5. **Bohula, E. A., A. J. Salisbury, M. Sohail, M. P. Playford, J. Riedemann, E. M. Southern, and V. M. Macaulay.** 2003. The efficacy of small interfering RNAs targeted to the type 1 insulin-like growth factor receptor (IGF1R) is influenced by secondary structure in the IGF1R transcript. J. Biol. Chem. **278:**15991–15997.
6. **Brack, K., I. Berk, T. Magulski, J. Lederer, A. Dotzauer, and A. Vallbracht.** 2002. Hepatitis A virus inhibits cellular antiviral defense mechanisms induced by double-stranded RNA. J. Virol. **76:**11920–11930.
7. **Chen, W., W. Yan, Q. Du, L. Fei, M. Liu, Z. Ni, Z. Sheng, and Z. Zheng.** 2004. RNA interference targeting VP1 inhibits foot-and-mouth disease virus replication in BHK-21 cells and suckling mice. J. Virol. **78:**6900–6907.
8. **Crowder, S., and K. Kirkegaard.** 2005. trans-dominant inhibition of RNA viral replication can slow growth of drug-resistant viruses. Nat. Genet. **37:** 701–707.
9. **de los Santos, T., Q. Wu, S. de Avila Botton, and M. J. Grubman.** 2005. Short hairpin RNA targeted to the highly conserved 2B nonstructural protein coding region inhibits replication of multiple serotypes of foot-and-mouth disease virus. Virology **335:**221–231.
10. **Egger, D., and K. Bienz.** 2005. Intracellular location and translocation of silent and active poliovirus replication complexes. J. Gen. Virol. **86:**707–718.
11. **Emerson, S. U., C. McRill, B. Rosenblum, S. Feinstone, and R. H. Purcell.** 1991. Mutations responsible for adaptation of hepatitis A virus to efficient growth in cell culture. J. Virol. **65:**4882–4886.
12. **Emerson, S. U., Y. K. Huang, C. McRill, M. Lewis, and R. H. Purcell.** 1992. Mutations in both the 2B and 2C genes of hepatitis A virus are involved in adaptation to growth in cell culture. J. Virol. **66:**650–654.
13. **Far R. K.-K., W. Nedbal, and G. Sczakiel.** 2001. Concepts to automate the theoretical design of effective antisense oligonucleotides. Bioinformatics **17:** 1058–1061.
14. **Flehmig, B., U. Heinricy, and M. Pfisterer.** 1990. Simultaneous vaccination for hepatitis A and B. J. Infect. Dis. **161:**865–868.
15. **Fuijwara, K., O. Yokosuka, F. Fukai, H. Imazeki, H. Saisho, and M. Omata.** 2001. Analysis of full-length hepatitis A virus genome in sera from patients with fulminant and self-limited acute type A hepatitis. J. Hepatol. **35:**112–119.
16. **Gauss-Müller, V., and Y. Kusov.** 2002. Replication of a hepatitis A virus replicon detected by genetic recombination in vivo. J. Gen. Virol. **83:**2183–2192.
17. **Geiss, B. J., T. C. Pierson, and M. S. Diamond.** 2005. Actively replicating West Nile virus is resistant to cytoplasmic delivery of siRNA. Virol. J. **2:**53–66.
18. **Giladi, H., M. Ketzinel-Gilad, L. Rivkin, Y. Felig, O. Nussbaum, and E. Galun.** 2003. Small interfering RNA inhibits hepatitis B virus replication in mice. Mol. Ther. **8:**769–776.
19. **Gitlin, L., S. Karelsky, and R. Andino.** 2002. Short interfering RNA confers intracellular antiviral immunity in human cells. Nature **418:**244–251.
20. **Gitlin, L., and R. Andino.** 2003. Nucleic acid-based immune system: the antiviral potential of mammalian RNA silencing. J. Virol. **77:**7159–7165.
21. **Gitlin, L., J. K. Stone, and R. Andino.** 2005. Poliovirus escape from RNA interference: short interfering RNA-target recognition and implications for therapeutic approaches. J. Virol. **79:**1027–1035.
22. **Haasnoot, P. C. J., D. Cupac, and B. Berkhout.** 2003. Inhibition of virus replication by RNA interference. J. Biomed. Sci. **10:**607–616.
23. **Heale, B. S., H. S. Soifer, C. Bowers, and J. J. Rossi.** 2005. siRNA target site secondary structure predictions using local stable substructures. Nucleic Acids Res. **33:**e30.
24. **Hohjoh, H.** 2002. RNA interference (RNAi) induction with various types of synthetic oligonucleotide duplexes in cultured human cells. FEBS Lett. **521:** 195–199.
25. **Holen, T., M. Amarzguioui, M. T. Wiiger, E. Babaie, and H. Prydz.** 2002. Positional effects of short interfering RNAs targeting the human coagulation trigger tissue factor. Nucleic Acids Res. **30:**1757–1766.
26. **Kanda, T., Y. Kusov, O. Yokosuka, and V. Gauss-Müller.** 2004. Interference of hepatitis A virus replication by small interfering RNAs. Biochem. Biophys. Res. Commun. **318:**341–345.
27. **Kanda, T., B. Zhang, Y. Kusov, O. Yokosuka, and V. Gauss-Müller.** 2005. Suppression of hepatitis A virus genome translation and replication by siRNAs targeting the internal ribosomal entry site. Biochem. Biophys. Res. Commun. **330:**1217–1223.
28. **Kapadia, S. B., A. Brideau-Andersen, and F. V. Chisari.** 2003. Interference of hepatitis C virus. RNA replication by short interfering RNAs. Proc. Natl. Acad. Sci. USA **100:**2014–2018.
29. **Kretschmer-Kazemi Far, R., and G. Sczakiel.** 2003. The activity of siRNA in mammalian cells is related to structural target accessibility: a comparison with antisense oligonucleotides. Nucleic Acids Res. **31:**4417–4424.
30. **Kronke, J., R. Kittler, F. Buchholz, M. P. Windisch, T. Pietschmann, R. Bartenschlager, and M. Frese.** 2004. Alternative approaches for efficient inhibition of hepatitis C virus RNA replication by small interfering RNAs. J. Virol. **78:**3436–3446.
31. **Kusov, Y., Y. A. Kazachkov, L. B. Elbert, G. I. Krutyanskaya, V. F. Poleschuk, A. V. Sobol, I. I. Titova, E. A. Lisitzina, S. G. Drozdov, and M. S. Balayan.** 1990. Characteristics of inactivated hepatitis A vaccine prepared from virus propagated in heteroploid continuous monkey cell line. Vaccine **8:**513–514.
32. **Kusov, Y., and V. Gauss-Müller.** 1999. Improving proteolytic cleavage at the 3A/3B site of the hepatitis A virus polyprotein impairs processing and particle formation, and the impairment can be complemented in *trans* by 3AB and 3ABC. J. Virol. **73:**9867–9878.
33. **Kusov, Y., R. Gosert, G. Dzagurov, G. Shatirishvili, M. Gerhardt, and V. Gauss-Müller.** 2004. Hepatitis A virus genome modified at its 3′terminus, p. 1–37. *In* C. R. Williams (ed.), Focus on genome research. Nova Biomedical Books, New York, N.Y.
34. **Kusov, Y., J. Heering, T. Kanda, O. Yokosuka, and V. Gauss-Müller.** 2004. Silencing of hepatitis A virus replication by RNA interference. Proc. 2nd Eur. Congr. Virol., Madrid, Spain, p. 77–85.
35. **Kusov, Y., R. Gosert, and V. Gauss-Müller.** 2005. Replication and in vivo repair of the hepatitis A virus genome lacking the poly(A) tail. J. Gen. Virol. **86:**1363–1368.
36. **Liu, M., W. Chen, Z. Ni., W. Yan, L. Fei, Y. Jiao, J. Zhang, Q. Du, X. Wei, J. Chen, Y. Liu, and Z. Zheng.** 2005. Cross-inhibition to heterologous foot-and-mouth disease virus infection induced by RNA interference targeting the conserved region of viral genome. Virology **336:**51–59.
37. **Lu, W. W., Y. Y. Hsu, J. Y. Yang, and S. H. Kung.** 2004. Selective inhibition of enterovirus 71 replication by short hairpin RNAs. Biochem. Biophys. Res. Commun. **325:**494–499.
38. **Luo, K. G., and D. C. Chang.** 2004. The gene-silencing efficiency of siRNA is strongly dependent on the local structure of siRNA at the targeted region. Biochem. Biophys. Res. Commun. **318:**303–310.
39. **McManus, M. T., C. P. Petersen, B. B. Haines, J. Chen, and P. A. Sharp.** 2002. Gene silencing using micro-RNA designed hairpins. RNA **8:**842–850.
40. **Merl, S., C. Michaelis, B. Jaschke, M. Vorpahl, S. Seidl, and R. Wessely.** 2005. Targeting 2A protease by RNA interference attenuates coxsackievirus cytopathogenicity and promotes survival in highly susceptible mice. Circulation **111:**1583–1592.
41. **Nakabayashi, H., K. Taketa, T. Yamane, M. Miyazaki, K. Miyano, and J. Sato.** 1984. Phenotypical stability of a human hepatoma cell line, Huh-7, in long-term culture with chemically defined medium. Gann **75:**151–158.
42. **Nykanen, A., B. Haley, and P. D. Zamore.** 2001. ATP requirement and small interfering RNA structure in the RNA interference pathway. Cell **107:**309–321.
43. **Overhof, M., M. Alken, R. Kretschmer-Kazemi Far, M. Lemaitre, B. Lebleu, G. Sczakiel, and I. Robbins.** 2005. Local RNA target structure influences siRNA efficacy: a systematic global analysis. J. Mol. Biol. **348:**871–881.
44. **Palmenberg, A. C., and J.-Y. Sgro.** 1997. Topological organization of picornaviral genomes: statistical prediction of RNA structural signals. Semin. Virol. **8:**231–241.
45. **Phipps, K. M., A. Martinez, J. Lu, B. A. Heinz, and G. Zhao.** 2004. Small interfering RNA molecules as potential anti-human rhinovirus agents: in vitro potency, specificity, and mechanism. Antivir. Res. **61:**49–55.
46. **Qiu, S., C. M. Adema, and T. Lane.** 2005. A computational study of off-target effects of RNA interference. Nucleic Acids Res. **33:**1834–1847.
47. **Rachow, A., V. Gauss-Müller, and C. Probst.** 2003. Homogenous hepatitis A virus particles, proteolytic release of the assembly signal 2A from procapsids by factor Xa. J. Biol. Chem. **278:**29744–29751.
48. **Saleh, M. C., R. P. Van Rij, and R. Andino.** 2004. RNA silencing in viral infections: insights from poliovirus. Virus Res. **102:**11–17.
49. **Schubert, S., A. Grünweller, V. A. Erdmann, and J. Kurreck.** 2005. Local RNA target structure influences siRNA efficacy: systematic analysis of intentionally designed binding regions. J. Mol. Biol. **348:**883–893.
50. **Taylor, J. A., and N. V. Naoumov.** 2005. The potential of RNA interference as a tool in the management of viral hepatitis. J. Hepatol. **42:**139–144.
51. **Vallbracht, A., L. Hofmann, K. G. Wurster, and B. Flehmig.** 1984. Persistent infection of human embryo fibroblasts by hepatitis A virus. J. Gen. Virol. **65:**609–615.
52. **Vento, S., T. Garofano, C. Renzini, F. Cainelli, F. Casali, G. Ghironzi, T. Ferraro, and E. Conzia.** 1998. Fulminant hepatitis A associated with hepatitis A virus superinfection in patients with chronic hepatitis C. N. Engl. J. Med. **338:**286–290.
53. **Vickers, T. A., S. Koo, C. F. Bennet, S. T. Crooke, N. M. Dean, and B. F.**

Baker. 2003. Efficient reduction of target RNAs by small interfering RNA and RNase H-dependent antisense agents. A comparative analysis. J. Biol. Chem. **278:**7108–7118.
54. **Vignuzzi, M., J. K. Stone, J. J. Arnold, C. E. Cameron, and R. Andino.** 2006. Quasispecies diversity determines pathogenesis through cooperative interaction in a viral population. Nature **439:**344–348.
55. **Westerhout, E. M., M. Ooms, M. Vink, A. T. Das, and B. Berkhout.** 2005. HIV-1 can escape from RNA interference by evolving an alternative structure in its RNA genome. Nucleic Acids Res. **33:**796–804.
56. **Wilson, J. A., and C. D. Richardson.** 2005. Hepatitis C virus replicons escape RNA interference induced by a short interfering RNA directed against the NS5b coding region. J. Virol. **79:**7050–7058.
57. **Yi, M., and S. M. Lemon.** 2002. Replication of subgenomic hepatitis A virus RNAs expressing firefly luciferase is enhanced by mutations associated with adaptation of virus to growth in cultured cells. J. Virol. **76:**1171–1180.
58. **Yu, J.-Y., J. Taylor, S. DeRuiter, A. B. Vojtek, and D. L. Turner.** 2003. Simultaneous inhibition of GSK3α and GSK3β using hairpin siRNA expression vectors. Mol. Ther. **7:**228–236.